The Astronomical Journal, 139:168–175, 2010 January doi:10.1088/0004-6256/139/1/168

ARECIBO MULTI-FREQUENCY TIME-ALIGNED PULSAR AVERAGE-PROFILE AND POLARIZATION DATABASE

Timothy H. Hankins[1] and Joanna M. Rankin[2]
[1] Physics Department, New Mexico Tech, Socorro, NM 87801, USA; thankins@nrao.edu
[2] Physics Department, University of Vermont, Burlington, VT 05401, USA; Joanna.Rankin@uvm.edu
Received 2008 April 3; accepted 2008 December 29; published 2009 December 10

ABSTRACT

We present Arecibo time-aligned, total intensity profiles for 46 pulsars over an unusually wide range of radio frequencies and multi-frequency, polarization-angle density diagrams, and/or polarization profiles for 57 pulsars at some or all of the frequencies 50, 111/130, 430, and 1400 MHz. The frequency-dependent dispersion delay has been removed in order to align the profiles for study of their spectral evolution, and wherever possible the profiles of each pulsar are displayed on the same longitude scale. Most of the pulsars within Arecibo's declination range that are sufficiently bright for such spectral or single pulse analysis are included in this survey. The calibrated single pulse sequences and average profiles are available by web download for further study.

Key words: polarization – pulsars: general

Online-only material: figure set

1. INTRODUCTION

As part of a program to study the geometrical constraints on the emission mechanism of pulsars, we present a set of total intensity average profiles at a number of frequencies from 25 to 4800 MHz at the Arecibo Observatory. The data were time-tagged so that through use of a suitable timing model for the pulsar, we were able to shift the arrival times of the pulses, modulo one stellar rotation period, to the solar system barycenter. Then by assuming a dispersion measure (DM) we shifted all the profiles to infinite frequency arrival time. In many cases, the DM was the only free parameter for alignment. The techniques used were similar to those of Hankins & Rickett (1986). In a few cases, our observations were coordinated with others made at the Pushchino Radio Astronomy Observatory (Hankins et al. 1991). In addition, we have observed a large overlapping group of pulsars at selected frequencies with full Stokes' parameters. We present these two sets of observations in a coordinated fashion, so that they can be used for studies of the pulsar magnetospheric structure. In several cases, where this polarimetry was incomplete, we have included profiles from older polarimetric observations.

Here we present these observations using three different kinds of analysis in order to introduce them to the pulsar community as a resource for future scientific use. They are available for download at http://www.uvm.edu/pulsar.

All three types of analysis and display have a long history at the Arecibo Observatory. As mentioned above, Hankins & Rickett (1986) pioneered this technique, and a further independent effort was made by Phillips & Wolszczan (1992). Programs of both average profile and individual pulse polarimetry using single channels began in 1971 at 430 MHz (e.g., Rankin et al. 1975; Rankin & Benson 1981), and at 1400 MHz after the first (1972–1974) Arecibo Observatory upgrade (Stinebring et al. 1984; Rankin et al. 1989), paving the way for the more sensitive and better resolved multi-channel observations reported here as well as the extensive and recent 1400 and 430 MHz polarization compendia by Weisberg et al. (1999, 2004). Stinebring et al. (1984), in particular, solved the vexing problem of correcting for cross-coupling errors in the polarimetry (see also Appendix A2). Finally, we display the polarimetry in two different ways: for weaker pulsars we show their average Stokes profiles, but for stronger ones we compute polarization-angle (hereafter PA) density displays similar in concept to those first presented by Backer & Rankin (1980).

Profile polarimetry programs have been carried out at other pulsar observatories: e.g., Jodrell Bank (e.g., Lyne et al. 1971; Gould & Lyne 1998); NRAO 300 ft (e.g., Manchester 1971); Parkes (Hamilton et al. 1977; McCulloch et al. 1978; Manchester et al. 1980; Johnston et al. 2006); Effelsberg (e.g., Morris et al. 1981; von Hoensbroech & Xilouris 1997); Pushchino (e.g., Suleimanova & Pugachev 2002) and most recently the Giant Metrewave Radio Telescope (India, GMRT, e.g., Johnston et al. 2008)—and many of these observations have been deposited for download at the European Pulsar Network Web site (http://www.mpifr-bonn.mpg.de/div/pulsar/data). However, within its declination range, the Arecibo Telescope's great sensitivity is often highly advantageous, especially for individual pulse polarimetry, although the GMRT in India now achieves comparable sensitivity at the lower frequencies (e.g., Mitra et al. 2007; Johnston et al. 2008).

2. OBSERVATIONS

The results of two main programs of time-aligned total-power and polarimetric pulse-sequence observations presented below were made at the Arecibo Observatory during a number of sessions between 1988 and 1992. A few observations from a previous polarimetric pulse-sequence survey at 430 MHz (J. M. Rankin & D. B. Campbell, unpublished; hereafter RC) and a subsequent one at 1400 MHz (Stinebring et al. 1984; hereafter SCRWB), however, are also included in order to extend the completeness of our coverage.[3]

[3] The observations were conducted under four different observing proposals with somewhat different objectives. Consequently, users of the online data should be aware that there are several formats for the data. Details are available with the online data.

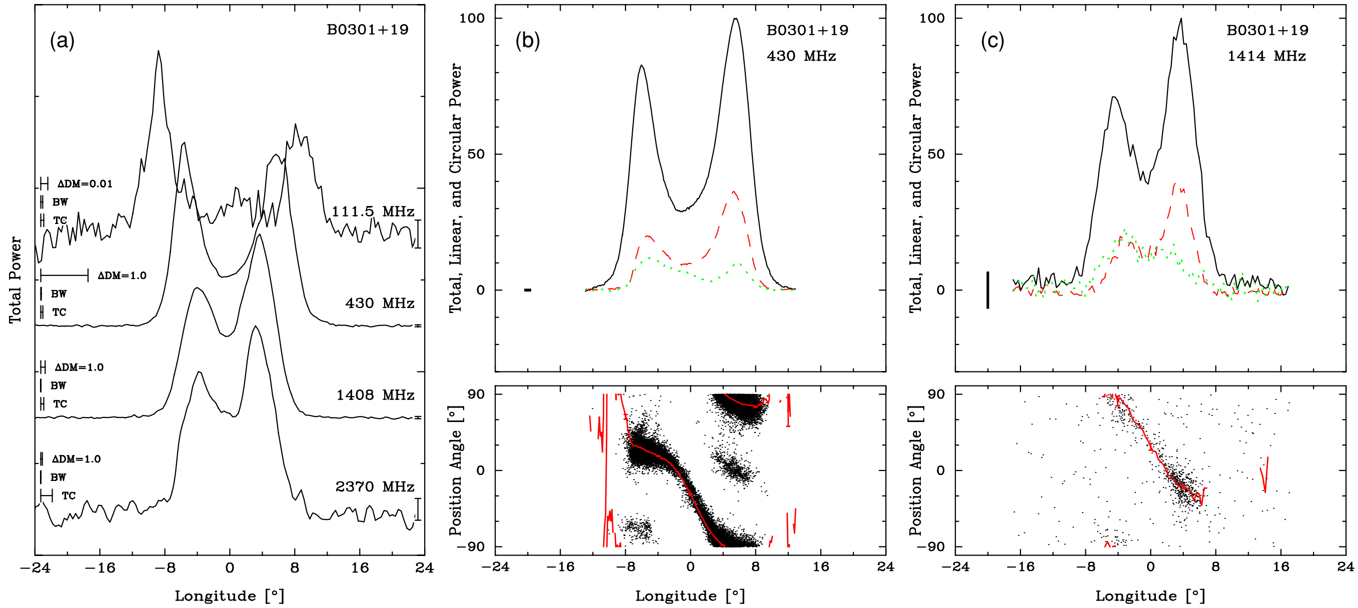

Figure 1. (a) Multi-frequency profiles, (b) the 430 MHz polarization histogram, and (c) the 1414 MHz polarization histogram for B0301+19.
(The complete figure set (64 images) is available in the online journal.)

2.1. Multiple Frequency Total Intensity Profiles

For the total intensity observation program, circularly polarized feeds were used at 430, 1400, 2370, and 4800 MHz and crossed-dipole linearly polarized feeds (with circular hybrids) were used at 26, 49, and 130/111 MHz. All profiles were obtained using the then existing Arecibo 40 MHz Correlator (Hagen 1987); the autocorrelation functions (ACFs) were accumulated into typically 1024 pulsar-synchronous phase bins spanning one pulsar period, and then written to tape every 2 minutes.

These ACFs were then Fourier transformed off-line to obtain power spectra, and the appropriate dispersion delays between adjacent spectral channels were removed. The profiles from all spectral channels were then coadded to produce a dedispersed average profile. The two-minute averages were edited to remove interference and other corruption, then synchronously added together to form (in many cases) a high signal-to-noise ratio average profile. The time tag of the first sample was used to relate the times of arrival to the solar system barycenter in terms of the pulsar phase at infinite frequency. Thus if the dispersion delays strictly obey the cold plasma dispersion law, then the pulses align in pulse phase exactly as they would if the observer were in the immediate pulsar neighborhood. The DM is, however, a free parameter in the phase alignment, and we found that adjustments from the tabulated values (Taylor et al. 1993; Manchester 2002) were required for optimal alignment for many of the pulsars. The DMs and timing models used for alignment are listed in Table 1.

To test and monitor the timing stability of the system during each observing session, we recorded a reference profile from a strong pulsar using the same sampling parameters each time. From these profiles systematic timing offsets could be determined and applied to data from other pulsars. Since it was not possible to observe throughout the whole range of frequencies in a single observing session, we recorded reference profiles for each pulsar, usually at 430 MHz, to confirm its tabulated timing model. In a number of cases, we had to make minor adjustments in the timing model to achieve alignments among profiles recorded at the same frequency; where applicable, these are indicated in the end notes of Table 1. After any timing issues were resolved, the DM was adjusted to obtain pulse-phase alignment among profiles at different frequencies. Since the change in pulse phase ϕ as a function of radio frequency ν, $d\phi/d\nu \propto \nu^{-3}$, we used the lowest frequency pairs with good signal-to-noise ratio to determine any adjustment to DM.

The fiducial point of a pulse profile to be used for inter-frequency alignment depends upon the pulse shape. Usually, aligning core components works well for pulsars with odd numbers of components. We aligned either the peak of the core component or the (symmetrical) half-power points for these pulsars. For double profiles, where the separation between the main components is clearly frequency dependent, we used the centroid between the two components.

2.2. Polarimetry

Most of the primary polarimetry observations were carried out during a set of sessions in 1992 October; a few, however, come from earlier observations in 1992 March and 1990 January. All used the then existing Arecibo 40 MHz Correlator, such that the average polarimetry was carried out in a continuous mode, whereas the pulse-sequence observations entailed use of special programs which gated the correlator synchronously with the pulsar. In both cases, the basic data recorded at the telescope were the auto- and cross-correlation functions of the left- and right-hand channel voltages. The 1400 MHz observations used a 20 MHz bandwidth and the lower a maximum of 10 MHz at 430 MHz, 2.5 MHz at 111/130 MHz, and 625 kHz at 49 MHz. A minimum of 32 correlation lags were retained in order to reduce the dispersion delay across the bandpass to usually negligible levels. The resolution was then often essentially the correlator dump time for the pulse-sequence observations and the averaging bin size for the profile-polarization measurements. These parameters are tabulated in Table 2. The Arecibo 40 MHz

Table 1
Alignment Periods, Period Derivatives, Reference Epoch, and Dispersion Measures

Pulsar	P (s)	$\dot{P} \times 10^{-15}$ (s s^{-1})	Epoch (MJD)	DM (pc cm^{-3})	Ephemeris References	Notes	Figure
B0301+19	1.3875836665891	1.29613	42325.500	15.650	C,C,C,C	a	A1.2(a)
B0523+11	0.354437595275	0.07362	48382.000	79.294	M,M,M,M		A1.3(a)
B0525+21	3.74549702041	40.0565	41993.500	51.024	C,C,C,C	b	A1.4(a)
B0540+23	0.2459740892957	15.42378	48382.000	77.698	M,M,M,M		A1.5(a)
B0611+22	0.33492505401	59.630	42881.000	96.86	M,M,M,H		A1.7(a)
B0626+24	0.476622653938	1.99705	48382.000	84.216	M,M,M,H	c	A1.8(a)
B0656+14	0.384885025950	55.0134	48423.000	14.02	M,M,M,M	d	A1.9(a)
B0751+32	1.44234944724	1.0802	43830.000	40.04	M,M,M,M	e	A1.10(a)
B0820+02	0.864872751896	0.10366	43419.347	23.6	M,M,M,M	f	A1.11(a)
B0823+26	0.53066061717618	1.714776	47165.705796	19.4750	Mc,Mc,Mc,H		A1.12(a)
B0834+06	1.273768080098	6.7995	48362.00	12.8579	H,M,M,H	g	A1.13(a)
B0919+06	0.43061431085	13.7248	43890.786	27.3091	H,T,T,T	h	A1.14(a)
B0940+16	1.08741772517	0.1	48500.00	20.5	M,M,M,H		A1.15(a)
B0943+10	1.097704890211	3.4884	45781.306	15.339	S,S,S,H	i	A1.16(a)
B0950+08	0.253065180710	0.229314	47165.7973	2.9701	Mc,Mc,Mc,H		A1.17(a)
B1133+16	1.187913314434	3.7341	47177.902	4.8472	Mc,Mc,Mc,H	j	A1.18(a)
B1237+25	1.38244915690	0.95954	47177.91	9.277	Mc,Mc,Mc,H	k	A1.19(a)
B1530+27	1.124835519553	0.803	46387.700	14.67	H,M,M,H		A1.20(a)
B1541+09	0.74844817748	0.43030	42304.00	34.99	T,T,T,T		A1.21(a)
B1604−00	0.4218162717899	0.30610	48419.00	10.6831	H,M,M,H		A1.22(a)
B1612+07	1.2068002120	2.357	43891.065	21.5	M,M,M,M		A1.23(a)
B1633+24	0.490506485351	0.1195	46075.099	24.265	M,M,M,H		A1.24(a)
B1737+13	0.803049715913	1.454	43892.616	48.73	H,M,M,H		A1.25(a)
B1821+05	0.752906449119	0.225	43890.159	66.7827	H,M,M,H		A1.26(a)
B1839+09	0.38131888145508	1.0916	43890.169	49.132	H,M,M,H		A1.27(a)
B1842+14	0.375462510949	1.866	43986.911	41.6	H,M,M,M		A1.28(a)
B1900+01	0.72930163274	4.0322	42345.50	245	M,M,M,H		A1.31
B1907+00	1.01694545765	5.5151	42647.00	111	M,M,M,M		A1.33
B1907+03	2.330260471	4.53	43984.933	83.5	M,M,M,H		A1.34
B1915+13	0.19462634149	7.20286	42302.00	94.494	T,T,T,M		A1.37(a)
B1918+19	0.82103460383	0.8952	42577.00	153.48	M,M,M,H		A1.39
B1919+21	1.337301192269	1.34809	40689.95	12.4309	M,M,M,M		A1.41(a)
B1920+21	1.07791915514	8.1899	42547.00	217.1	M,M,M,M		A1.42(a)
B1929+10	0.226517153473	1.15675	41704.00	3.176	H,T,T,T		A1.44(a)
B1933+16	0.358736247894	6.00354	42265.00	158.53	H,M,M,M		A1.45(a)
B1944+17	0.44061846173	0.02404	41501.00	16.11	T,T,T,M		A1.46(a)
B1952+29	0.426676786488	0.00164	48415.00	7.86	M,M,M,H		A1.49(a)
B2016+28	0.557953408114	0.14720	40688.50	14.1965	C,C,C,H	l	A1.52(a)
B2020+28	0.343401720116	1.8935	47018.182	24.623	H,M,M,H		A1.53(a)
B2044+15	1.1382856067	0.185	43890.254	39.71	M,M,M,H		A1.56(a)
B2110+27	1.202851149957	2.6225	46075.294	25.122	H,M,M,H		A1.59(a)
B2113+14	0.440152954660	0.290	43986.016	56.14	H,M,M,H		A1.60(a)
B2210+29	1.00459237450	0.4948	46074.83	74.6	M,M,M,H		A1.62(a)
B2303+30	1.575884744270	2.89567	42341.00	49.575	M,M,M,H	m	A1.63(a)
B2315+21	1.444652673768	1.05	43987.099	20.865	H,M,M,H	n	A1.64(a)

Notes.
[a] B0301+19: 2370 MHz profile is shifted by −6.17 ms to correct systematic offset; see Section 2.1.
[b] B0525+21: 2370 MHz profile is shifted by −7.32 ms to correct systematic offset; see Section 2.1.
[c] B0626+24: 2370 MHz and 430 MHz profiles are shifted by 9.25 and 40.91 ms to correct systematic offset; see Section 2.1. DM is determined from 1408 to 111.5 MHz alignment. The "bump" preceding the 430 MHz pulse at longitude $-18°$ is probably spurious. In a few cases, the correlator failed to start at the correct time and thus misaligned certain individual two-minute scans. Most of these faults were corrected at an earlier point in our reduction, but this "bump" was not noticed until after the constituent two-minute scans had been destroyed.
[d] B0656+14: 430 MHz profile is shifted by −11.29 ms to correct systematic offset; see Section 2.1.
[e] B0751+32: arbitrary alignment by profile centroids; see Section 2.1.
[f] B0820+02: arbitrary alignment by profile centroids; see Section 2.1.
[g] B0834+06: 2370 MHz profile is shifted by 8.40 ms to correct systematic offset; see Section 2.1.
[h] B0919+06: 4880 and 111.5 MHz profiles are shifted by −1.42 and −9.93 ms to correct systematic offsets; see Section 2.1.
[i] B0943+10: the two 111.5 MHz profiles in the multi-frequency display, showing the two modes of B0943+10, were recorded 1 year apart. They align well using Shabanova's (1990) timing model. The 430 and 24.8 MHz profiles, recorded 4 days apart, also align well, so the DM determination is based on this frequency pair. Then these two profiles are shifted by 5.92 ms to align with the 111.5 MHz profiles, and the 49.2 MHz profile is arbitrarily shifted by 26.1 ms to align its centroid.
[j] B1133+16: 49.2 MHz profile is shifted by −9.48 ms to correct systematic offset; see Section 2.1.

Table 1
(Continued)

[k] B1237+25: 4880 MHz profile shifted by 15.1 ms to correct systematic offset; see Section 2.1.
[l] B2016+28: the dramatic pulse shape change between 111.5 and 430 MHz is consistently observed on different days. The DM used for alignment was adjusted to align the 49.2 and 111.5 MHz profile peaks, though if the profile is actually bifurcating at low frequencies, this alignment may be incorrect. We have searched the literature in an effort to see if any other very low frequency profile could settle this bifurcation question, but apparently our 50 MHz observation is the only published profile below 100 MHz.
[m] B2303+30: 4880 and 1408 MHz profiles are shifted by −39.40 ms to correct systematic offset; see Section 2.1.
[n] B2315+21: 2370 MHz profile is shifted by −37.12 ms to correct systematic offset; see Section 2.1.
References. The ephemeris reference keys refer to the sources of P, $\dot{P}$, Epoch, and DM, respectively. C: J. M. Cordes (1992, private communication); H: this work; M: Manchester et al. (2002); Mc: M. M. McKinnon (1990, private communication); T: Taylor et al. (1993); S: Shabanova (1990).

Correlator is described by Hagen (1987) and the continuous and gated observing software by Perillat (1988) and P. Perillat (1992, private communication). The measured correlation functions were scaled, three-level-sampling corrected, and Fourier transformed to produce raw Stokes parameters, which were in turn corrected (channel by channel) for dispersion, Faraday rotation, instrumental delays, and all of the known feed imperfections as determined by full-sky tracks of pulsar B1929+10 and other sources. These methods are more completely described in Appendix A2. During the course of our analyses, we discovered that the instrumental polarization is highly frequency dependent, particularly at 430 MHz; therefore, the most recent observations represent some of the best calibrated ever made at the Arecibo Observatory. For some few, however, not all of the calibration information was available for one reason or another. We found, for instance, that interference rather easily corrupted our continuum-source observations, which are needed to determine the relative left- and right-hand channel gains, for calibration of the circular polarization V. In any case, Table 2 indicates this gain calibration with a "c" when a continuum source was used and "n" when computed from the off-pulse noise level. The correction of the Stokes parameters for cross-coupling in the feed is denoted by a "p."

Profile and single-pulse polarimetry were also carried out during these three sessions at 111.5 or 130 MHz and near 50 MHz. The techniques were virtually identical to those described above except that additional corrections were required for the changing ionospheric Faraday rotation, and many fewer of our efforts to obtain reliable feed cross-coupling data were successful.

The older 430 MHz observations were carried out in the early 1970s with a single-channel polarimeter using various bandwidths and integration times as appropriate for the particular star being observed and tabulated in Table 2. The polarimetry scheme is described in Rankin et al. (1975), and while the nominal 0.25% voltage amplitude of the feed cross-coupling, which can produce spurious circular polarization at typical levels of about 10% of the linear polarization, was known from radar observations, correction of the Stokes parameters was then impossible because the cross-coupling phase was unknown.

The older 1400 MHz observations were carried out in 1981 October, again with a single-channel, adding polarimeter. Here, the bandwidths ranged up to 40 MHz, with these and the integration times chosen to provide a resolution of about a milliperiod. A serious effort was made for the first time to correct the measured Stokes parameters for instrumental cross-coupling distortion using the "orthogonal" approximation described by Stinebring et al. (1984).

In all cases, we make no effort to give absolute polarization position angles. Therefore, the position angles in our polarization displays are arbitrary within a constant value.

Generally, our polarimetric analyses used the then existing tabulated rotation measures (RM) on the ATNF Web site (Manchester 2002). However, in a few cases we were able to measure new RM where they were then unknown. These were determined in the course of our polarimetric analyses by fitting the polarization position-angle swing across the available bandwidth. The errors in the RM values were computed from the position-angle errors which in turn were computed from the off-pulse noise level and represent one standard deviation. The values are given in boldface with their errors in Table 2. The value for B1919+14 remains a new determination, whereas the other five generally agree within their errors with values determined since. No effort was made to correct for the effect of ionospheric Faraday rotation, either on the estimated errors of measured RM or in the processing using the tabulated interstellar values; however, at Arecibo this contribution typically is no larger than ± 1 rad m^2, thus well within the stated errors.

3. RESULTS

Our results are summarized in the tables and figures. Table 1 gives the period, period derivative, timing epoch and DM value used for the multi-frequency alignments, and Table 2 gives the observation date, configuration, resolution and RM values used in the polarimetric analyses.

The combined multi-frequency and polarimetry results are presented in right ascension order in Figures A1.1–A1.64 in order to facilitate intercomparison. When available, the multi-frequency profiles are presented first, followed by polarization plots from the available frequencies. Details of the multi-frequency alignments and polarimetry are given in Tables 1 and 2.

The time resolution of the multi-frequency profiles is indicated by a set of three horizontal bars plotted on the left side of the profiles. The upper bar denotes the phase shift which would result from a change of DM of 0.01, 0.1, or 1.0 pc cm^{-3}. The middle bar, labeled "BW" shows the time resolution limited by the dispersion sweep time, $\tau_{\rm DM} = {\rm DM}\,\Delta\nu/(1.205\times 10^{-16}\nu^3)$, across the receiver bandwidth, $\Delta\nu$, tuned to frequency ν. The bottom bar shows the integration time constant used for the plot. An error bar is plotted on the left side of the multi-frequency profile plots to show the range of two standard deviations of the off-pulse noise fluctuations.

For the polarization plots the total intensity, linear, and circular polarizations are depicted by solid, dashed, and dotted

Table 2
Polarimetry Configuration, Calibration and Rotation Measure

Pulsar	Date	Frequency (MHz)	Bandwidth (MHz)	Channels	Calibration[a]	Resolution (deg)	RM[b] (rad m^{-2})	Figure
B0045+33	1992 Oct 16	430.0	10.0	32	cp	0.40		A1.1(a)
B0301+19	1974 Jan 05	430.0	2.0	1	c	0.85	−8.3	A1.2(b)
	1992 Oct 20	1414.0	20.0	32	cp	0.31		A1.2(c)
B0523+11	1992 Oct 17	430.0	1.25	32	cp	0.41	78.7	A1.3(b)
	1992 Oct 20	1414.0	20.0	32	cp	0.41		A1.3(c)
B0525+21	1974 Apr 01	430.0	2.0	1	c	2.76	50.96	A1.4(b)
	1981 Oct 11	1404.0	20.0	1	c	0.15		A1.4(c)
B0540+23	1974 Jan 05	430.0	0.1	1	c	1.19	77.58	A1.5(b)
	1992 Oct 20	1414.0	20.0	32	cp	0.38		A1.5(c)
B0609+37	1992 Oct 17	430.0	5.0	32	cp	0.53	8.5	A1.6(a)
B0611+22	1992 Oct 19	430.0	5.0	32	cp	0.85	67.0	A1.7(b)
	1992 Oct 20	1414.0	20.0	32	cp	0.38		A1.7(c)
B0626+24	1992 Feb 16	430.0	10.0	64	cp	1.06	82.0	A1.8(b)
	1992 Oct 20	1414.0	20.0	32	cp	0.31		A1.8(c)
B0656+14	1992 Feb 12	430.0	10.0	32	cp	0.43	22.0	A1.9(b)
	1992 Feb 17	1414.0	20.0	32	cp	0.37		A1.9(c)
B0751+32	1992 Dec 19	430.0	10.0	32	cp	0.32	−7.0	A1.10(b)
B0820+02	1992 Oct 19	430.0	10.0	32	cp	0.36	13.0	A1.11(b)
	1992 Oct 20	1414.0	20.0	32	cp	0.36		A1.11(c)
B0823+26	1992 Oct 20	430.0	10.0	32	cp	0.43	5.9	A1.12(b)
	1992 Oct 15	1414.0	20.0	32	cp	0.34		A1.12(c)
B0834+26	1992 Feb 16	49.3	0.63	2.6	n	0.70	3.9	A1.13(b)
	1992 Oct 15	111.5	2.5	1.8	n	0.70		A1.13(c)
	1974 Apr 01	430.0	2.0	1	c	0.76		A1.13(d)
	1992 Oct 15	1414.0	20.0	1	cp	0.22		A1.13(e)
B0919+06	1992 Feb 17	49.2	0.31	2.6	n	2.00	27.25	A1.14(b)
	1992 Feb 15	132.0	2.5	1.8	n	1.61		A1.14(c)
	1992 Oct 20	430.0	10.0	32	cp	0.74		A1.14(d)
	1981 Oct 11	1404.0	20.0	1	cp	0.68		A1.14(e)
B0940+16	1992 Oct 17	430.0	10.0	32	cp	0.35	53.0	A1.1(b)
B0943+10	1990 Jan 17	111.5	2.5	64		1.18	13.3	A1.16(b)
	1992 Oct 19	430.0	10.0	32	cp	0.33		A1.16(c)
B0950+08	1992 Feb 15	49.3	0.63	1.8	n	2.00	2.969	A1.17(b)
	1971 Nov 06	430.0	10.0	1	cp	0.88		A1.17(c)
	1981 Oct 10	1404.0	20.0	1	cp	0.28		A1.17(d)
B1133+13	1992 Feb 16	49.5	0.63	1.8	n	0.50	3.9	A1.18(b)
	1990 Jan 17	111.5	1.25	1.8	n	0.70		A1.18(c)
	1992 Oct 19	430.0	10.0	32	cp	0.31		A1.18(d)
	1992 Oct 16	1414.0	20.0	32	cp	0.37		A1.18(e)
B1237+25	1992 Feb 15	132.0	2.5	64		0.35	9.296	A1.19(b)
	1974 Jan 06	430.0	10.0	32	cp	0.50		A1.19(c)
	1981 Oct 11	1404.0	20.0	32	cp	0.10		A1.19(d)
B1541+09	1992 Feb 14	130.0	2.5	2.6		1.15	21.0	A1.21(b)
	1990 Jan 17	430.0	10.0	32	cp	1.45		A1.21(c)
B1604−00	1992 Feb 14	130.0	2.5	1.8		1.20	6.5	A1.22(b)
	1973 Feb 11	430.0	10.0	1	c	1.91		A1.22(c)
B1737+13	1992 Oct 20	430.0	10.0	32	cp	0.71	73.0	A1.25(b)
	1992 Oct 24	1414.0	20.0	32	cp	0.36		A1.25(c)
B1821+05	1990 Jan 05	430.0	5.0	64	cp	0.34	145.0	A1.26(b)
	1992 Oct 19	1414.0	20.0	32	cp	0.36		A1.26(c)
B1839+09	1992 Oct 23	1414.0	20.0	32	cp	0.38	53.0	A1.27(b)
B1842+14	1992 Oct 23	1414.0	20.0	32	cp	0.39	121.0	A1.28(b)
B1845−01	1992 Oct 24	1414.0	20.0	32	cp	0.39	580.0	A1.29(a)
B1859+03	1992 Oct 18	1414.0	20.0	32	cp	0.66	−237.4	A1.30(a)
B1900+05	1992 Oct 24	1414.0	20.0	32	cp	0.37	−113.0	A1.32(a)
B1907+10	1973 Oct 21	430.0	0.05	1	c	0.98	540.0	A1.35(b)
	1992 Oct 24	1414.0	20.0	32	cp	0.51		A1.36(c)
B1910+20	1992 Feb 15	430.0	10.0	64	cp	0.35	148.0	A1.36(a)
B1915+13	1973 Sep 07	430.0	0.1	1	c	1.82	233.0	A1.37(b)
	1992 Oct 22	1414.0	20.0	32	cp	0.33		A1.37(c)
B1917+00	1974 May 08	430.0	0.5	1	c	1.34	...	A1.38(a)
B1919+14	1992 Oct 20	430.0	5.0	64	cp	0.44	**275.0 ± 60.0**	A1.40(a)
B1919+21	1990 Jan 05	430.0	10.0	32	cp	0.19	37.0	A1.41(b)
	1992 Oct 22	1414.0	20.0	32	cp	0.33		A1.41(c)

Table 2
(Continued)

Pulsar	Date	Frequency (MHz)	Bandwidth (MHz)	Channels	Calibration[a]	Resolution (deg)	RM[b] (rad m^{-2})	Figure
B1920+21	1992 Oct 19	1414.0	20.0	32	cp	0.34	282.0	A1.42(a)
B1923+04	1990 Jan 6	430.0	5.0	32		0.55	−37.0	A1.43(a)
B1929+10	1974 Dec 24	430.0	2.0	1	cp	1.05	−6.1	A1.44(b)
	1992 Oct 18	1414.0	20.0	32	cp	0.49		A1.44(c)
B1933+16	1973 Jul 24	430.0	0.1	1	c	1.16	−1.9	A1.45(a)
B1944+17	1973 Jul 27	430.0	2.0	1	c	2.78	−28.0	A1.46(b)
	1992 Oct 23	1414.0	20.0	32	cp	0.33		A1.46(c)
B1946+35	1974 May 8	430.0	0.25	1	c	1.69	−78.0	A1.47(b)
	1992 Oct 18	1414.0	20.0	32	cp	0.33		A1.47(c)
B1951+32	1990 Jan 4	1414.0	20.0	32	cp	2.81	−113.0	A1.48(a)
B1952+29	1990 Feb 15	430.0	10.0	32	cp	0.35	−18.0	A1.49(b)
B2000+32	1992 Oct 20	430.0	5.0	64	cp	1.03	20.0	A1.50(b)
B2002+32	1973 Jul 28	430.0	0.25	1		1.04	30.0	A1.51(a)
	1992 Oct 22	1414.0	20.0	32	cp	0.34		A1.51(b)
B2016+28	1992 Oct 15	430.0	10.0	32	cp	0.39	−34.6	A1.52(b)
	1992 Oct 18	1414.0	20.0	32	cp	0.39		A1.52(c)
B2020+28	1992 Oct 16	430.0	10.0	32	cp	0.43	−74.8	A1.53(b)
	1992 Oct 18	1414.0	20.0	32	cp	0.37		A1.53(c)
B2028+22	1992 Oct 26	430.0	5.0	64	cp	0.40	**−195.0 ± 25.0**	A1.54(a)
B2034+19	1992 Oct 26	430.0	10.0	32	cp	0.35	**−98.5 ± 8.0**	A1.55(a)
B2044+15	1992 Feb 14	430.0	10.0	64	cp	0.40	−101.0	A1.56(b)
	1992 Oct 19	1414.0	20.0	32	cp	0.32		A1.56(c)
B2053+21	1992 Oct 20	430.0	10.0	64	cp	0.35	**−100.0 ± 7.0**	A1.57(a)
	1992 Oct 18	1414.0	20.0	32	cp	0.35		A1.57(b)
B2053+36	1992 Oct 24	1414.0	20.0	32	cp	0.66	−68.0	A1.58(a)
B2110+27	1992 Feb 14	430.0	10.0	32	cp	0.35	−65.0	A1.59(b)
	1992 Oct 22	1414.0	20.0	32	cp	0.30		A1.59(c)
B2113+14	1992 Oct 29	430.0	5.0	32	cp	0.74	−25.0	A1.60(b)
	1992 Oct 23	1414.0	20.0	32	cp	0.37		A1.60(c)
B2122+13	1992 Oct 16	430.0	10.0	32	cp	0.51	**−48.3 ± 3.6**	A1.61(a)
B2210+29	1992 Oct 16	430.0	10.0	32	cp	0.43	**−175.3 ± 15.**	A1.62(b)
	1992 Oct 23	1414.0	20.0	32	cp	0.36		A1.62(c)
B2303+30	1992 Oct 22	130.0	2.5	1.8	c	0.84	−84.0	A1.63(b)
	1992 Oct 15	430.0	10.0	32	cp	0.37		A1.63(c)
	1981 Oct 11	1414.0	20.0	32	cp	0.28		A1.63(d)
B2315+21	1992 Feb 14	430.0	10.0	32	cp	0.35	−37.0	A1.64(b)
	1992 Oct 19	1414.0	20.0	32	cp	0.35		A1.64(c)

Notes.
[a] Gain calibration obtained from observations of a standard continuum source is indicated by “c”. “n” indicates that the gain calibration is based on the off-pulse noise level. Correction of the Stokes parameters for cross-coupling in the antenna feed is denoted by “p.”
[b] For the observations at 50 MHz, 111.5 MHz, and 130 MHz, a search was carried out over a large range of rotation measure to maximize the linear polarization before combining the individual frequency channels, and the successive two-minute scans were rotated to a common PA before combining them. This was found necessary because of a changing effective RM with time. The boldface RM values were determined in the course of this work and are given with their estimated errors; whereas the other values were taken from the ATNF pulsar catalog (http://www.atnf.csiro.au/research/pulsar/psrcat/). No effort was made to correct for the ionospheric Faraday rotation, either in processing or in specifying the RM errors, which is typically less that 1 rad m^2.

lines, respectively. The solid vertical bars indicate the range of three standard deviations of the off-pulse noise. Where present, the time resolution, including the effects of dispersion across the receiver band and the post-integration time constant are shown by a horizontal bar. In the lower part of each polarization plot, the average linear polarization position angle is shown wherever the linear polarization exceeds two times the off-pulse noise fluctuations.

Error bars for the position angle are shown for $\pm 3\sigma$ uncertainties due to the estimation error of the linear polarization. For many of the pulsars individual pulse records were available. For these pulsars the position angle of each sample which exceeded two times the off-pulse noise is plotted as a dot. This type of plot allows study of polarization moding behavior (Manchester et al. 1975; Backer & Rankin 1980).

4. DOWNLOADS

Data files corresponding to the pulse sequences and profiles presented in this paper are available for download at http://www.uvm.edu/pulsar along with Fortran 77 codes for reading them. Complete explanations of the data formats are given as comments in these codes. If these observations and codes are used in future publications, we ask that reference be made to this paper.

5. DESCRIPTION OF APPENDICES

Appendix A1. The first Appendix consists of plots of the average profiles and polarimetry of the 64 pulsars in our study,

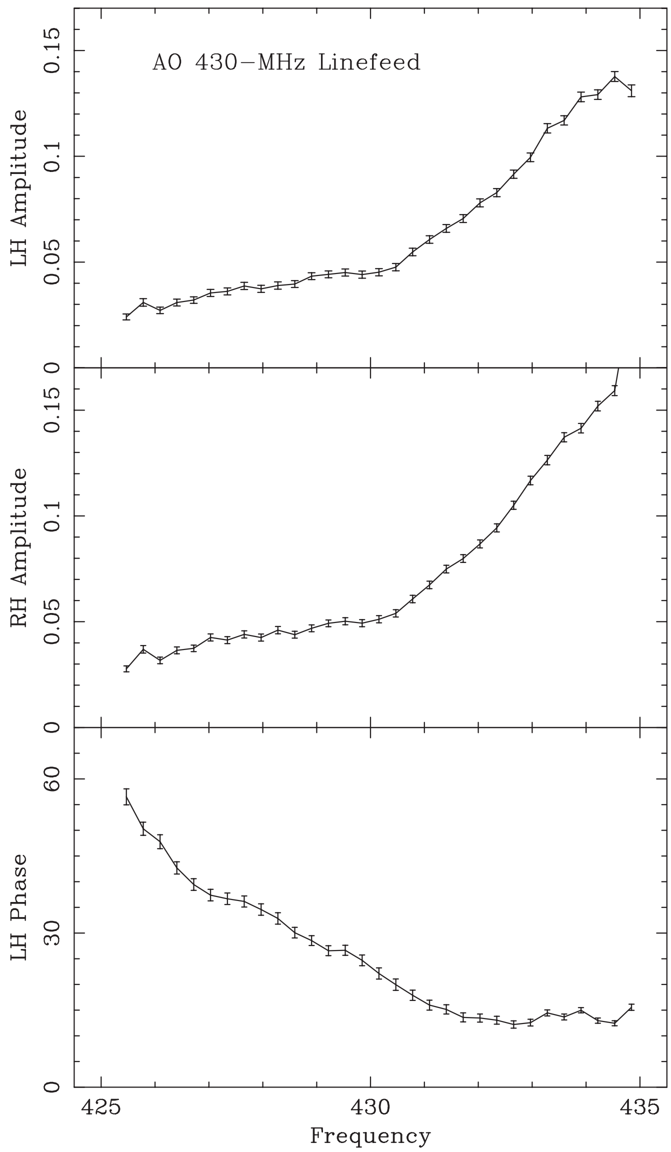

Figure A2.1. Left-hand (top panel) and right-hand (middle panel) cross-coupling amplitudes and the left-hand cross-coupling phase (bottom panel) as a function of frequency for the Arecibo Observatory 430 MHz line feed as determined from a full-sky track of pulsar B1929+10 in 1992 October. The right-hand phase is orthogonal to the plotted left-hand phase within the observational errors, which represent one standard deviation.

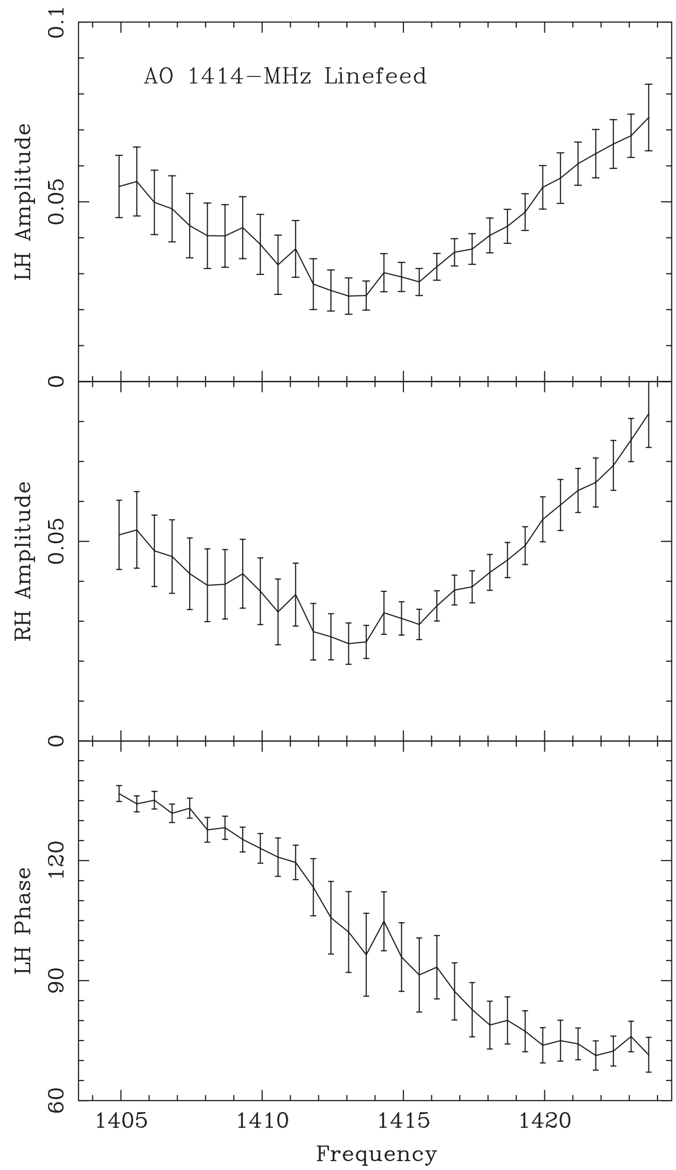

Figure A2.2. Cross-coupling amplitudes and phase for the Arecibo Observatory 1400 MHz line feed, determined from a full-sky track of pulsar B1929+10 in 1992 October, as in Figure A2.1.

Figures A1.1–A1.64 (available in the online journal). We show Figure 1 here as typical of the sample.

The multi-frequency average profiles are time-aligned (see Section 2.1) and displayed in ascending-frequency order. Polarization histograms are used to display the individual-pulse polarization properties. Polarization profiles present the average-polarization observations.

Both the polarization histograms and the polarized profile displays have two panels with the total power (Stokes I), total linear polarization ($L \equiv \sqrt{Q^2 + U^2}$), and circular polarization (Stokes V, defined as right-hand minus left-hand circular polarization) in the upper panel, and the PA (PA $\equiv \tan^{-1}(U/Q)$) in the lower panel. The polarization histograms show the PA density of the individual samples that exceed an appropriate $>3\sigma$ threshold (see Section 3) with the average PA overplotted (red curve). Both the total linear (L, dashed red) and circular (V, dotted green) polarization curves are shown in color, and by contrast, the polarization profile displays are shown in black and white. In both types of display, a small box at the left of the upper panel gives the resolution and a deflection corresponding to two off-pulse noise standard deviations.

Appendix A2. A summary of the polarimetric calibration procedures used is given in Appendix A2. The results of the cross-coupling analysis of the Arecibo 430 MHz and 1414 MHz line feeds are shown in Figures A2.1 and A2.2. These results were used to correct the measured Stokes parameters whenever possible.

We wish to acknowledge Dan Stinebring's assistance in making many of the profile observations as well as making available some of our 1981 polarimetry and that of Amy Carlow, Vera Izvekova, N. Rathnasree, Svetlana Suleymanova, and Kyriaki Xilouris in carrying out some of the 1990/1992 observations. It is a pleasure to thank Phil Perillat without whose remarkable software for the Arecibo 40 MHz Correlator this work would have been impossible. We thank Mark McKinnon of NRAO for determining timing models for many of these pulsars, Dipanjan Mitra for alignment of some of the profiles, the Pushchino pulsar group of the Lebedev Physical Institute for 61 and 102 MHz profiles, and J. A. Phillips for the 25 MHz profiles. The Arecibo Observatory is part of the National Astronomy and Ionosphere Center, which is operated by Cornell University for the National Science Foundation. This material is based upon work supported by the National Science Foundation under grants AST-8917722, AST-9618408, AST-9986754 and AST-0139641.

REFERENCES

Backer, D. C., & Rankin, J. M. 1980, ApJS, 42, 143
Gould, D. M., & Lyne, A. G. 1998, MNRAS, 301, 235
Hagen, J. 1987, NAIC Electronics Department Manual No. 8319
Hamilton, P. A., McCulloch, P. M., Ables, J. G., & Komesaroff, M. M. 1977, MNRAS, 180, 1
Hankins, T. H., Izvekova, V. A., Malofeev, V. M., Rankin, J. M., Shitov, Yu. P., & Stinebring, D. R. 1991, ApJ, 373, 17
Hankins, T. H., & Rickett, B. J. 1986, ApJ, 311, 684
Johnston, S., Hobbs, G., Vigeland, S., Kramer, M., Weisberg, J. M., & Lyne, A. G. 2006, MNRAS, 364, 1397
Johnston, S., Karastergiou, A., Mitra, D., & Gupta, Y. 2008, MNRAS, 388, 261
Lyne, A. G., Smith, F. G., & Graham, D. A. 1971, MNRAS, 153, 377
Manchester, R. N. 1971, ApJS, 23, 283
Manchester, R. N. 2002, www.atnf.csiro.au/research/pulsar/psrcat
Manchester, R. N., Hamilton, P. A., & McCulloch, P. M. 1980, MNRAS, 192, 153
Manchester, R. N., Taylor, J. H., & Huguenin, G. R. 1975, ApJ, 86, 418
McCulloch, P. M., Hamilton, P. A., Manchester, R. N., & Ables, J. G. 1978, MNRAS, 183, 645
Mitra, D., Rankin, J. M., & Gupta, Y. 2007, MNRAS, 379, 932
Morris, D., Graham, D. A., Sieber, W., Bartel, N., & Thomasson, P. 1981, A&AS, 46, 421
Perillat, P. 1988, NAIC Computer Department Report No. 23
Phillips, J. A., & Wolszczan, A. 1992, ApJ, 385, 273
Rankin, J. M., & Benson, J. M. 1981, AJ, 346, 869
Rankin, J. M., Campbell, D. B., & Spangler, S. R. 1975, NAIC Report No. 46
Rankin, J. M., Stinebring, D. R., & Weisberg, J. M. 1989, ApJ, 346, 869
Shabanova, T. V. 1990, Sov. Astron., 34, 269
Stinebring, D. R., Cordes, J. M., Rankin, J. M., Weisberg, J. M., & Boriakoff, V. 1984, ApJS, 55, 247 (SCRWB)
Suleimanova, S. A., & Pugachev, V. D. 2002, Astron. Rep., 46, 309
Taylor, J. H., Manchester, R. N., & Lyne, A. G. 1993, ApJS, 88, 529
von Hoensbroech, A., & Xilouris, K. M. 1997, A&AS, 126, 121
Weisberg, J. M., Cordes, J. M., Kuan, B., Devine, J. E., Green, J. T., & Backer, D. C. 2004, ApJS, 150, 317
Weisberg, J. M., et al. 1999, ApJS, 121, 171